



A numerical approach for solving nonlinear Fredholm integro-differential equation with boundary layer

Musa Cakir¹ · Yilmaz Ekinci² · Erkan Cimen³

Received: 17 March 2022 / Revised: 21 May 2022 / Accepted: 31 May 2022 /
Published online: 23 July 2022

© The Author(s) under exclusive licence to Sociedade Brasileira de Matemática Aplicada e Computacional 2022

Abstract

The study deals with an initial-value problem for a singularly perturbed nonlinear Fredholm integro-differential equation. Parameter explicit theoretical bounds on the continuous solution and its derivative are derived. To solve the approximate solution to this problem, a new difference scheme is constructed with the finite difference method by using the interpolated quadrature rules with the remaining terms in integral form. Parameter uniform error estimates for the approximate solution are established. It is proved that the method converges in the discrete maximum norm, uniformly with respect to the perturbation parameter. Numerical results are given to illustrate the parameter-uniform convergence of the numerical approximations.

Keywords Singular perturbation · Initial-value problem · Fredholm integro-differential equation · Uniform convergence · Shishkin mesh

Mathematics Subject Classification 65L05 · 65L11 · 65L12 · 65L20 · 65R20

Communicated by Hui Liang.

Musa Cakir and Yilmaz Ekinci have contributed equally to this work.

✉ Erkan Cimen
cimenerkan@hotmail.com

Musa Cakir
cakirmusa@hotmail.com

Yilmaz Ekinci
ylmz_eknc@hotmail.com

¹ Department of Mathematics, Faculty of Science, Van Yuzuncu Yil University, Van 65080, Turkey

² Department of Mathematics, Institute of Natural and Applied Sciences, Van Yuzuncu Yil University, Van 65080, Turkey

³ Department of Mathematics, Faculty of Education, Van Yuzuncu Yil University, Van 65080, Turkey

1 Introduction

Fredholm integro-differential equations (FIDEs) serve as mathematical models in many fields of science and engineering. FIDEs arise in fluid dynamics, physics, electro dynamics of complex medium, economics, biological models, epidemic models, many models of population growth, neural network modeling, oscillation theory, astronomy, chemistry, heat and mass transfer, theory of elasticity (Amiraliyev et al. 2020; Emamzadeh and Kajani 2010; Jerri 1999). In general, it is usually quite difficult to obtain exact solution of FIDEs. Because of this reason we need suitable discretization methods with high accuracy for solving FIDEs.

In this work, we deal with a singularly perturbed nonlinear Fredholm integro-differential equation (SPNFIDE) as follows:

$$\varepsilon u'(t) + f(t, u(t)) + \lambda \int_0^T K(t, s, u(s)) ds = 0, \quad t \in I = (0, T], \quad (1)$$

$$u(0) = A, \quad (2)$$

where $0 < \varepsilon \ll 1$ is the perturbation parameter, A is given constant, λ is a real parameter, $f(t, u)((t, u) \in \bar{I} \times R)$ and $K(t, s, u)((t, s, u) \in \bar{I} \times \bar{I} \times R)$ are sufficiently smooth functions, $\bar{I} = [0, T]$. Furthermore,

$$\frac{\partial f}{\partial u} \geq \alpha > 0.$$

Under these assumptions, there exist a unique solution u to problem (1)–(2). Besides, the existence and uniqueness studies of the solutions of nonlinear FIDEs can be found in Jerri (1999), O'Regan and Meehan (1998) and reference therein.

Singularly perturbed problems involve a small perturbation parameter, ε multiplied with the highest-order derivative terms. Such problems arise in applications of mathematics to problems in numerous fields of sciences and engineering. Theory of plates, semi-conductor device models, fluid mechanics, in fluid flow at high Reynolds number, quantum mechanics, reaction–diffusion processes, elasticity, etc. are among these. Due to the presence of boundary layers, the solution of these types of problems vary suddenly in boundary layers when ε approaches zero. In regions outside the layers, the solution behaviors regularly and varies slowly (Cakir and Arslan 2021; Cimen and Cakir 2017; Doolan et al. 1980; Farrell et al. 2000; Miller et al. 2012; Nayfeh 1993; O'Malley 1991; Roos et al. 2008).

In the last decades, there has received much attention in the numerical solution of integral equations. In literature, there are many different numerical models to solve such equations. Ebrahimi and Rashidina (Ebrahimi and Rashidinia 2015) presented a collocation method for solving linear and nonlinear Fredholm and Volterra integral equations, using the globally defined B-spline and auxiliary basis functions. Wang et al. Wang et al. (2019) studied on numerical solution of integro-differential equations of high-order Fredholm by the simplified reproducing kernel method. Maleknejad and Attary Maleknejad and Attary (2011) given Cattani's method based on the collocation approach for solving linear FIDEs. Emamzadeh and Kajani Emamzadeh and Kajani (2010) proposed a numerical approach to solve the nonlinear Fredholm integral equations of the second kind. Najafi Najafi (2020) introduced Nyström-quasilinearization method for solving nonlinear weakly singular Fredholm integral equations. Asgari et al. Asgari et al. (2019) studied on an iterative method to solve one- and two-dimensional linear Fredholm integral equations.

The above-mentioned articles, related to Fredholm integral equations were only concerned with the regular cases (i.e., when the boundary layers are absent). Studies on singularly perturbed Fredholm integro-differential equations (SPFIDEs) have attracted attention in recent years (Amiraliyev et al. 2018, 2020; Cimen and Cakir 2021; Durmaz and Amiraliyev 2021). However, although there are many studies on linear SPFIDEs in the literature, we could not find any studies on nonlinear SPFIDEs. These gaps in the literature are the motivation for our study. In addition, methods such as Reproducing kernel method, Fourier spectral method and Barycentric interpolation collocation method presented for the solution of the nonlinear singularly perturbed problems have recently attracted attention (Han and Wang 2022; Han et al. 2022; Liu et al. 2018).

In this article, we try to develop an efficient fitted difference scheme on Shishkin mesh for the numerical solution of the problem (1)–(2). The difference scheme is constructed by the method of integral identities with the use of appropriate interpolating quadrature rules with remainder terms in integral form.

The outline of the paper is organized as follows. In Sect. 2, we indicate the asymptotic behavior of the exact solution and its derivative. In Sect. 3, we construct the finite difference method and describe a special piecewise uniform mesh. Convergence and error analysis of the difference discretization are presented in Sect. 4. Some numerical examples are given in Sect. 5, which demonstrate the efficiency and the proposed method.

Throughout the paper, C denotes a generic positive constant. Some specific, fixed constants of this kind are indicated by subscripting C . For any continuous function $g(t)$, we use $\|g\|_\infty$ for the continuous maximum norm on the corresponding interval.

2 Bound of the exact solution and its derivative

In this section, we give bound of the exact solution and its derivative, which are needed in later sections for the analysis of appropriate numerical solution.

Lemma 1 *Suppose that the following assumptions are fulfilled*

$$\begin{aligned} \frac{\partial^m f}{\partial t^m}, \frac{\partial^n f}{\partial u^n} \in C^1(\bar{I} \times R), \frac{\partial^m K}{\partial t^m}, \frac{\partial^n K}{\partial s^n}, \frac{\partial^k K}{\partial u^k} \\ \partial u^k \in C^1(\bar{I} \times \bar{I} \times R); m, n, k = 0, 1 \end{aligned} \tag{3}$$

and

$$|\lambda| < \frac{\alpha}{\max_{0 \leq t \leq T} \int_0^T |G(t, s)| ds}$$

Then, the solution $u(t)$ of the problem (1)–(2) satisfies the estimates

$$\|u\|_\infty \leq C_0, \tag{4}$$

and

$$|u'(t)| \leq C \left\{ 1 + \frac{1}{\varepsilon} e^{-\frac{\alpha t}{\varepsilon}} \right\}, 0 \leq t \leq T, \tag{5}$$

where

$$C_0 = \frac{|A| + \alpha^{-1} \|q\|_\infty}{1 - \alpha^{-1} |\lambda| \max_{0 \leq t \leq T} \int_0^T |G(t, s)| ds},$$

$$G(t, s) = \frac{\partial}{\partial u} K(t, s, \gamma u), 0 < \gamma < 1,$$

$$q(t) = -f(t, 0) - \lambda \int_0^T K(t, s, 0) ds.$$

Proof We first prove (4). Applying the mean value theorem to the functions in (1), we have

$$\varepsilon u'(t) + p(t)u(t) + \lambda \int_0^T G(t, s)u(s)ds = q(t), t \in I, \tag{6}$$

where

$$p(t) = \frac{\partial}{\partial u} f(t, \theta u), 0 < \theta < 1.$$

From the Eq. (6), we can write the following form:

$$\begin{aligned} |u(t)| &\leq |u(0)| e^{-\frac{1}{\varepsilon} \int_0^t p(\eta) d\eta} + \frac{1}{\varepsilon} \int_0^t |q(\tau)| e^{-\frac{1}{\varepsilon} \int_\tau^t p(\eta) d\eta} d\tau \\ &\quad + \frac{|\lambda|}{\varepsilon} \int_0^t \left[\int_0^T |G(t, s)| |u(s)| ds \right] e^{-\frac{1}{\varepsilon} \int_\tau^t p(\eta) d\eta} d\tau \\ &\leq |A| e^{-\frac{\alpha t}{\varepsilon}} + \frac{\|q\|_\infty}{\varepsilon} \int_0^T e^{-\frac{\alpha(t-\tau)}{\varepsilon}} d\tau \\ &\quad + \frac{|\lambda|}{\varepsilon} \int_0^t \left[\int_0^T |G(t, s)| |u(s)| ds \right] e^{-\frac{\alpha(t-\tau)}{\varepsilon}} d\tau. \end{aligned}$$

From here, we take

$$\begin{aligned} \|u\|_\infty &\leq |A| + \alpha^{-1} \|q\|_\infty \left(1 - e^{-\frac{\alpha t}{\varepsilon}}\right) \\ &\quad + \alpha^{-1} |\lambda| \left(1 - e^{-\frac{\alpha t}{\varepsilon}}\right) \|u\|_\infty \max_{0 \leq t \leq T} \int_0^T |G(t, s)| ds, \end{aligned}$$

which proves (6).

To prove (5), differentiating Eq. (1) we have

$$\varepsilon u''(t) + b(t)u'(t) = F(t), \tag{7}$$

where

$$b(t) = \frac{\partial}{\partial u} f(t, u),$$

and

$$F(t) = -\frac{\partial}{\partial t} f(t, u) - \lambda \int_0^T \frac{\partial}{\partial t} K(t, s, u(s)) ds.$$

From the relations (3) and (4), we have

$$|F(t)| \leq C. \tag{8}$$

Using (1), we can obtain

$$|u'(0)| \leq \frac{|f(0, A)|}{\varepsilon} + \frac{|\lambda|}{\varepsilon} \int_0^T |K(0, s, u(s))| ds \leq \frac{C}{\varepsilon}. \tag{9}$$

It follows from (7) that

$$\begin{aligned} |u'(t)| &\leq \frac{C}{\varepsilon} e^{-\frac{\alpha t}{\varepsilon}} + \frac{\|F\|_\infty}{\varepsilon} \int_0^T e^{-\frac{\alpha(t-\tau)}{\varepsilon}} d\tau \\ &\leq \frac{C}{\varepsilon} e^{-\frac{\alpha t}{\varepsilon}} + \alpha^{-1} \|F\|_\infty \left(1 - e^{-\frac{\alpha t}{\varepsilon}}\right). \end{aligned}$$

Thus we arrive at (5). □

3 Discretization and Mesh

To give an approximation of the (1)–(2), we integrate (1) over (t_{i-1}, t_i) :

$$\begin{aligned} \varepsilon u_{\bar{t},i} + h_i^{-1} \int_{t_{i-1}}^{t_i} f(t, u) dt + h_i^{-1} \lambda \int_{t_{i-1}}^{t_i} \left[\int_0^T K(t, s, u) ds \right] dt = 0, \end{aligned} \tag{10}$$

where $u_{\bar{t},i} = (u_i - u_{i-1})/h_i$, $u_i = u(t_i)$ and $h_i = t_i - t_{i-1}$ for $1 \leq i \leq N$.

If integration by parts is applied to identity (10), we then obtain the relation

$$\varepsilon u_{\bar{t},i} + f(t_i, u_i) + \lambda \int_0^T K(t_i, s, u(s)) ds + R_i^{(1)} + R_i^{(2)} = 0, \tag{11}$$

where the remainder terms are

$$R_i^{(1)} = -h_i^{-1} \int_{t_{i-1}}^{t_i} (\xi - t_{i-1}) \frac{d}{d\xi} f(\xi, u(\xi)) d\xi, \tag{12}$$

and

$$R_i^{(2)} = -\lambda h_i^{-1} \int_{t_{i-1}}^{t_i} (\xi - t_{i-1}) \frac{d}{d\xi} \left(\int_0^T K(\xi, s, u(s)) ds \right) d\xi. \tag{13}$$

For integral term involving kernel function, using the composite right-side rectangle rule, we obtain the relation as follows:

$$\lambda \int_0^T K(t_i, s, u(s)) ds = \lambda \sum_{j=1}^N h_j K(t_i, s_j, u_j) + R_i^{(3)}, \tag{14}$$

with

$$R_i^{(3)} = \lambda \sum_{j=t_{i-1}}^N \int_{t_{j-1}}^{t_j} (t_{j-1} - \xi) \frac{d}{d\xi} K(t_i, \xi, u(\xi)) d\xi. \tag{15}$$

By the relations (10), (11) and (14) for $u(t_i)$, we get the following exact relation:

$$\varepsilon u_{\bar{t},i} + f(t_i, u_i) + \lambda \sum_{j=1}^N h_j K(t_i, s_j, u_j) + R_i = 0, i = 1, 2, \dots, N, \tag{16}$$

$$u_0 = A, \tag{17}$$

where the remainder term R_i is defined by

$$R_i = R_i^{(1)} + R_i^{(2)} + R_i^{(3)}. \tag{18}$$

Neglecting R_i in (16), we may suggest the following difference scheme for approximating (1)–(2):

$$\varepsilon y_{\bar{t},i} + f(t_i, y_i) + \lambda \sum_{j=1}^N h_j K(t_i, s_j, y_j) = 0, i = 1, 2, \dots, N, \tag{19}$$

$$y_0 = A. \tag{20}$$

The difference scheme (19)–(20) to be ε -uniformly convergent in what follows we will use the fitted piecewise uniform mesh (Shishkin type mesh). For the even number N , Shishkin-type mesh divides each of the interval $[0, \sigma]$ and $[\sigma, T]$ into $N/2$ equidistant subintervals. The transition point σ which separates of fine and coarse portions of the mesh is defined by

$$\sigma = \min \left\{ \frac{T}{2}, \alpha^{-1} \varepsilon \ln N \right\}.$$

We denote the stepsizes in there subintervals as follows:

$$h = \frac{2\sigma}{N}, H = \frac{2(T - \sigma)}{N},$$

$$h \leq lN^{-1}, lN^{-1} \leq H \leq 2lN^{-1}, h + H = 2lN^{-1}.$$

The mesh points of ω_N are being defined by

$$\omega_N = \begin{cases} t_i = ih, i = 1, 2, \dots, N/2, \\ t_i = \sigma + (i - \frac{N}{2})H, i = N/2 + 1, \dots, N. \end{cases}$$

and $\bar{\omega}_N = \omega_N \cup \{t_0 = 0\}$.

4 Uniform error estimates

To investigate the convergence of the method, note that $z_i = y_i - u_i$ ($0 \leq i \leq N$) is the solution of the following discrete problem:

$$\begin{aligned} \varepsilon z_{i,i} + [f(t_i, y_i) - f(t_i, u_i)] \\ + \lambda \sum_{j=1}^N h_i [K(t_i, s_j, y_j) - K(t_i, s_j, u_j)] = R_i, 1 \leq i \leq N, \end{aligned} \tag{21}$$

$$z_0 = 0. \tag{22}$$

Lemma 2 Under the conditions of Lemma 1, for the remainder term R_i of the scheme (19)–(20), the estimate

$$\|R\|_{\infty, \omega_N} \leq CN^{-1} \ln N \tag{23}$$

holds.

Proof We first consider the relation (12). Taking into account (4) and (5) in (12), then we have the inequality

$$\begin{aligned} |R_i^{(1)}| &\leq h_i^{-1} \int_{t_{i-1}}^{t_i} (\xi - t_{i-1}) \left[\left| \frac{\partial}{\partial \xi} f(\xi, u(\xi)) \right| + \left| \frac{\partial}{\partial u} f(\xi, u(\xi)) \right| |u'(\xi)| \right] d\xi \\ &\leq h_i^{-1} \int_{t_{i-1}}^{t_i} (\xi - t_{i-1}) |1 + u'(\xi)| d\xi \\ &\leq C \left\{ h_i + \int_{t_{i-1}}^{t_i} |u'(\xi)| d\xi \right\}, i = 1, 2, \dots, N. \end{aligned} \tag{24}$$

Next we analyze the relation (13). Taking into account (4) in (13), we get the inequality

$$\begin{aligned} |R_i^{(2)}| &\leq |\lambda| h_i^{-1} \int_{t_{i-1}}^{t_i} (\xi - t_{i-1}) \left| \frac{d}{d\xi} \int_0^T K(\xi, s, u(s)) ds \right| d\xi \\ &\leq |\lambda| h_i^{-1} \int_{t_{i-1}}^{t_i} (\xi - t_{i-1}) \int_0^T \left| \frac{\partial}{\partial \xi} K(\xi, s, u(s)) \right| ds d\xi \\ &\leq Ch_i, i = 1, 2, \dots, N. \end{aligned} \tag{25}$$

Finally, we denote the relation (15). By (4) and (5) in (15), we can write the following inequality:

$$\begin{aligned}
 |R_i^{(3)}| &\leq |\lambda| \sum_{j=l_{i-1}}^N \int_{t_{j-1}}^{t_j} (t_{j-1} - \xi) \left| \frac{\partial}{\partial \xi} K(t_i, \xi, u(\xi)) + \frac{\partial}{\partial u} K(t_i, \xi, u(\xi)) u'(\xi) \right| d\xi \\
 &\leq C \sum_{j=l_{i-1}}^N \int_{t_{j-1}}^{t_j} (t_{j-1} - \xi) |1 + u'(\xi)| d\xi \\
 &\leq C \max_{1 \leq j \leq N} h_j \int_{t_{i-1}}^{t_i} |1 + u'(\xi)| d\xi, \quad i = 1, 2, \dots, N.
 \end{aligned}
 \tag{26}$$

Thus, substituting the inequalities (24), (25) and (26) in (18), we obtain

$$|R_i| \leq C \left\{ h_i + \int_{t_{i-1}}^{t_i} |u'(\xi)| d\xi \right\}, \quad i = 1, 2, \dots, N.
 \tag{27}$$

In the first case, we consider that $\sigma = \frac{T}{2}$, $\frac{T}{2} < \alpha^{-1} \varepsilon \ln N$ and $h = H = TN^{-1}$. From (27) we take

$$\begin{aligned}
 |R_i| &\leq C \int_{t_{i-1}}^{t_i} (1 + \varepsilon^{-1}) dt = Ch(1 + \varepsilon^{-1}) \\
 &\leq C \frac{T}{N} \left(1 + \frac{2}{T} \alpha^{-1} \ln N \right).
 \end{aligned}
 \tag{28}$$

It follows from (28) that

$$|R_i| \leq CN^{-1} \ln N, \quad i = 1, \dots, N.
 \tag{29}$$

In the second case, we consider $\sigma = \alpha^{-1} \varepsilon \ln N$, and so $\alpha^{-1} \varepsilon \ln N < \frac{T}{2}$. We estimate R_i on $[0, \sigma]$ and $[\sigma, T]$, separately. In the boundary layers $[0, \sigma]$, inequality (27) reduces to

$$|R_i| \leq C(1 + \varepsilon^{-1})h \leq C(2\alpha^{-1} \varepsilon N^{-1} \ln N + 2\alpha^{-1} N^{-1} \ln N).$$

Hence,

$$|R_i| \leq CN^{-1} \ln N, \quad \text{for } i = 1, \dots, \frac{N}{2}.
 \tag{30}$$

We now estimate the remainder term R_i in the region $[\sigma, T]$. From (27), we take

$$|R_i| \leq C \left\{ H + \int_{t_{i-1}}^{t_i} |u'(t)| dt \right\}.$$

Taking into account (5) here, we have

$$|R_i| \leq C \left\{ H + \alpha^{-1} \left(e^{-\frac{\alpha t_{i-1}}{\varepsilon}} - e^{-\frac{\alpha t_i}{\varepsilon}} \right) \right\}.
 \tag{31}$$

Since

$$t_i = \alpha^{-1} \varepsilon \ln N + \left(i - \frac{N}{2}\right) H,$$

we obtain

$$e^{-\frac{\alpha t_i}{\varepsilon}} = e^{-\frac{\alpha}{\varepsilon} \left[\alpha^{-1} \varepsilon \ln N + \left(i - \frac{N}{2}\right) H\right]} = N^{-1} e^{-\frac{\alpha}{\varepsilon} \left(i - \frac{N}{2}\right) H} \leq N^{-1} \tag{32}$$

and

$$e^{-\frac{\alpha t_{i-1}}{\varepsilon}} = e^{-\frac{\alpha}{\varepsilon} \left[\alpha^{-1} \varepsilon \ln N + \left(i-1 - \frac{N}{2}\right) H\right]} = N^{-1} e^{-\frac{\alpha}{\varepsilon} \left(i-1 - \frac{N}{2}\right) H} \leq N^{-1}. \tag{33}$$

Substituting (32) and (33) into (31), we have

$$|R_i| \leq C \{2TN^{-1} + \alpha^{-1}N^{-1}\}.$$

Hence, it follows that

$$|R_i| \leq CN^{-1}, \text{ for } i = \frac{N}{2} + 1, \dots, N. \tag{34}$$

Combining the estimates (29), (30) and (34), we arrive at (23). □

Lemma 3 *If we assume the condition*

$$|\lambda| < \frac{\alpha}{\max_{1 \leq i \leq N} \sum_{j=1}^N h_i |G_{ij}|},$$

then for the solution of the difference problem (21)–(22) the following estimate holds:

$$\|z\|_\infty \leq \alpha^{-1} \left(1 - \alpha^{-1} |\lambda| \max_{1 \leq i \leq N} \sum_{j=1}^N h_i |G_{ij}|\right)^{-1} \|R\|_\infty. \tag{35}$$

Proof Applying the mean value theorem to function in (21), we get

$$\varepsilon z_{\bar{i},i} + a_i z_i + \lambda \sum_{j=1}^N h_i G_{ij} = R_i, \quad 1 \leq i \leq N,$$

where

$$a_i = \frac{\partial}{\partial u} f(t_i, u_i + \theta z_i)$$

and

$$G_{ij} = \frac{\partial}{\partial u} K(t_i, s_j, u_j + \theta z_j), \quad 0 < \theta < 1.$$

According to maximum principle for the operator $\varepsilon z_{\bar{i},i} + a_i z_i$, we can write

$$\|z\|_\infty \leq \alpha^{-1} \|R\|_\infty + \alpha^{-1} |\lambda| \|z\|_\infty \max_{1 \leq i \leq N} \sum_{j=1}^N h_i |G_{ij}|,$$

which immediately lead to (35). □

Finally, we obtain the main results for this work.

Table 1 The resulting errors $e^{\varepsilon, N}$ and e^N , convergence rates p^N for test problem

ε	$N = 64$	$N = 128$	$N = 256$	$N = 512$	$N = 1024$
2^{-2}	0.0095961 0.93	0.0050309 0.97	0.0025761 0.98	0.0013037 0.99	0.0006559
2^{-4}	0.0096366 0.72	0.0058458 0.77	0.0034276 0.81	0.0019566 0.84	0.0010963
2^{-6}	0.0095653 0.72	0.0058027 0.77	0.0034023 0.81	0.0019421 0.84	0.0010882
2^{-8}	0.0095479 0.72	0.0057921 0.77	0.0033961 0.81	0.0019386 0.84	0.0010862
2^{-10}	0.0095436 0.72	0.0057895 0.77	0.0033946 0.81	0.0019377 0.84	0.0010857
2^{-12}	0.0095425 0.72	0.0057889 0.77	0.0033942 0.81	0.0019375 0.84	0.0010856
2^{-14}	0.0095422 0.72	0.0057887 0.77	0.0033941 0.81	0.0019375 0.84	0.0010856
2^{-16}	0.0095422 0.72	0.0057887 0.77	0.0033941 0.81	0.0019375 0.84	0.0010856
e^N	0.0096366	0.0058458	0.0034276	0.0019566	0.0010963
p^N	0.72	0.77	0.81	0.84	

Theorem 1 Under the conditions of Lemma 1, the solution of (1)–(2) and the solution (13)–(14) satisfy the estimate

$$\|y - u\|_{\infty, \bar{\omega}_N} \leq CN^{-1} \ln N. \tag{36}$$

Proof Combining the previous lemmas, we immediately arrive at (36). □

5 Algorithm and numerical results

5.1 Algorithm

In this section, we present the following iterative technique for solving nonlinear problem (19)–(20).

$$y_i^{(n)} = \frac{A_i y_{i-1}^{(n)} + B_i y_i^{(n-1)} - C_i - D_i}{\frac{\varepsilon}{h_i} + \frac{\partial}{\partial y} f(t_i, y_i^{(n-1)}) + \lambda h_i \frac{\partial}{\partial y} K(t_i, s_i, y_i^{(n-1)})}, \quad i = 1, 2, \dots, N,$$

$$y_0^{(n)} = A,$$

where

$$A_i = \frac{\varepsilon}{h_i}, \quad B_i = \frac{\partial}{\partial y} f(t_i, y_i^{(n-1)}) + \lambda h_i \frac{\partial}{\partial y} K(t_i, s_i, y_i^{(n-1)}),$$

$$C_i = f(t_i, y_i^{(n-1)}) + \lambda h_i K(t_i, s_i, y_i^{(n-1)}),$$

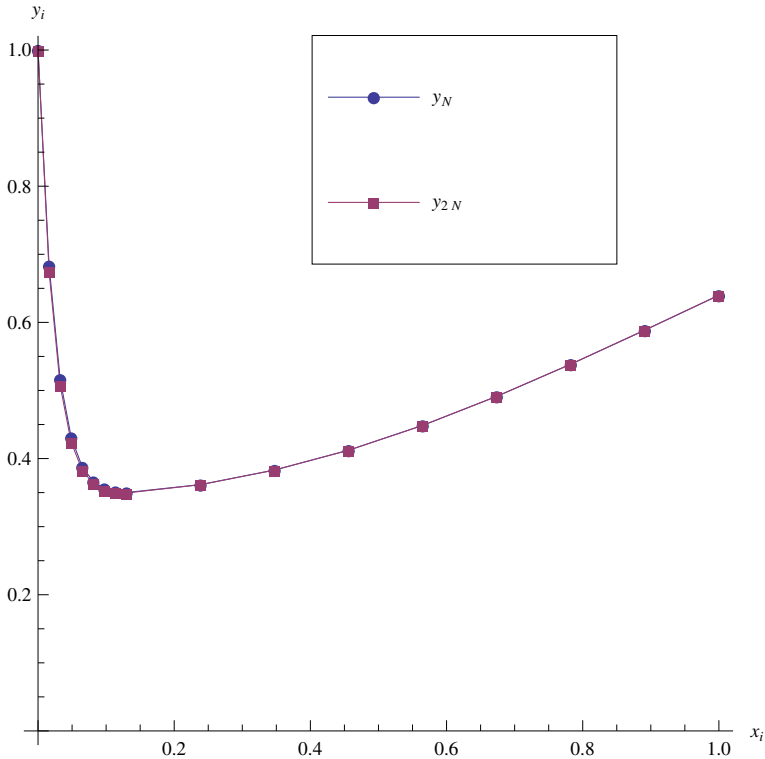


Fig. 1 Numerical results of test problem for $N = 64$ and $\varepsilon = 2^{-4}$

$$D_i = \lambda \sum_{j=1}^N h_j \left[K(t_i, s_j, y_j^{(n-1)}) + \frac{\partial}{\partial y} K(t_i, s_j, y_j^{(n-1)}) \times (y_j^{(n)} - y_j^{(n-1)}) \right], i \neq j,$$

$$D_i = 0, \text{ for } i = j,$$

$n = 1, 2, \dots$, and $y_i^{(0)}$ is given.

5.2 Numerical example

We consider SPNFIDE in the form:

$$\varepsilon u'(t) + 2u(t) + \tanh(u(t)) + \frac{1}{4} \int_0^1 t^2 \sin(u(s)) ds + e^t = 0, 0 < t \leq 1,$$

$$u(0) = 1.$$

As the exact solution $u(t)$ of this problem unknown. Therefore, we use the double-mesh principle to approximate the maximum errors on our mesh $\bar{\omega}_N$. That is, we compare the computed solutions with the solution on a mesh that is twice as fine (Doolan et al. 1980; Farrell et al. 2000). The initial guess used here is taken as $y_i^{(0)} = 1 - e^{-t_i}$ and the number of iterations n is chosen such that

$$\max_i |y_i^{(n)} - y_i^{(n-1)}| \leq 10^{-5}.$$

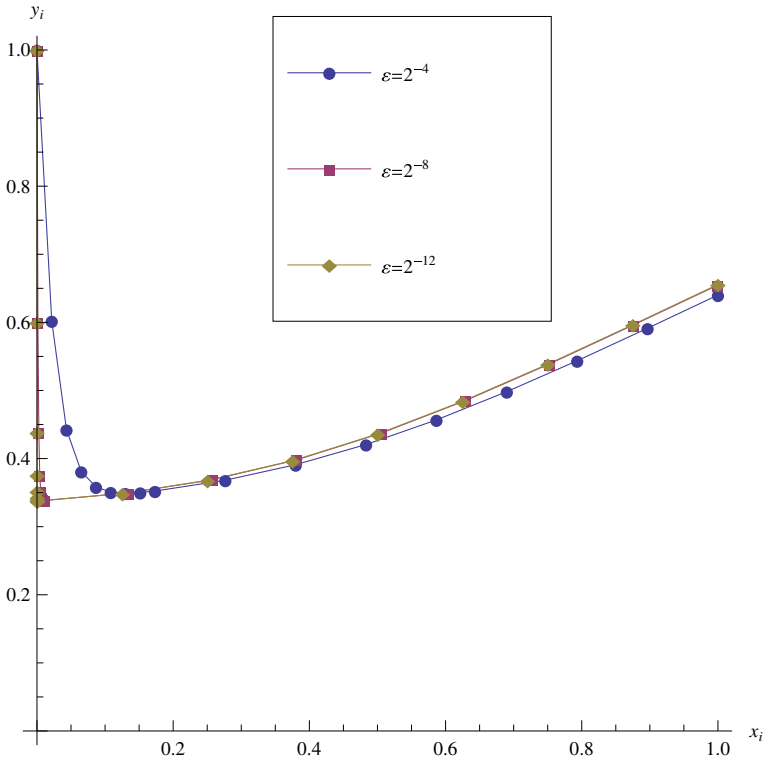


Fig. 2 Numerical results of test problem for $N = 256$ and various ε

The two mesh difference is denoted by

$$e^{\varepsilon, N} = \max_{\omega_N} \left| y^{\varepsilon, N} - \tilde{y}^{\varepsilon, 2N} \right|,$$

where $\tilde{y}^{\varepsilon, 2N}$ is the numerical which comprises points of the original mesh $t_i \in \omega_N$ and their midpoints $t_{i+1/2} = (t_i + t_{i+1})/2, i = 0, 1, \dots, N - 1$.

Thus, the maximum errors are taken as

$$e^N = \max_{\varepsilon} e^{\varepsilon, N}.$$

In addition, the orders of convergence and the ε -uniform rates of convergence are defined as

$$p^{\varepsilon, N} = \ln(e^{\varepsilon, N} / e^{\varepsilon, 2N}) / \ln 2, p^N = \ln(e^N / e^{2N}) / \ln 2.$$

The resulting errors $e^{\varepsilon, N}$ and the orders of convergence $p^{\varepsilon, N}$ for particular values of ε and N , are listed in the Table 1.

To validate the applicability of the method, one test problem is considered for numerical experimentation for different values of the perturbation parameter and mesh points. The numerical results are listed in terms of the approximate errors, the rates of convergence (see Table 1). Further, behavior of the numerical solution (see Figs. 1, 2) and the ε -uniform convergence of the method is shown by the log-log plot (see Fig. 3). From the results in the table, we observe that the maximum pointwise errors (e^N) decreases monotonically and the

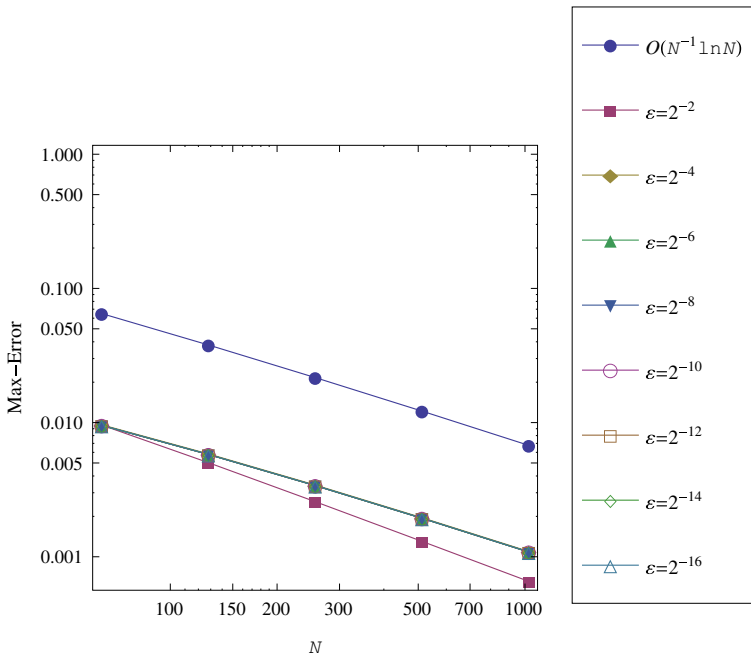


Fig. 3 Maximum point-wise errors of log–log plot for test problem

rates of convergence (p^N) increases monotonically when the number of mesh points (N) increases. From Figs. 1 and 2, we observe that the solution of the example exhibit a boundary layer $t = 0$. And from Fig. 3, we notice that the maximum pointwise errors are bounded by $O(N^{-1} \ln N)$, which is proved in Theorem 1.

6 Conclusion

The singularly perturbed initial-value problem for a nonlinear first-order Fredholm integro-differential equation is considered. To solve this problem, a fitted difference scheme on a piecewise uniform mesh was presented. First order convergence except for a logarithmic factor, in the discrete maximum norm, independently of the perturbation parameter was obtained. The computed errors and rates of convergence were displayed in Table 1 and plotted Figs. 1, 2, 3 for the considered test problem, which supported of the theoretical results. These results showed that the presented method was effective and accuracy. We point out that the presented method in this article can be extended to other type of initial or boundary value problems such as nonlinear SPFIDEs, reaction diffusion SPFIDEs.

Acknowledgements The authors are grateful in advance to the referees and the editors for their valuable comments and suggestions which helped to improve the quality of manuscript.

Data availability Data sharing is not applicable to this article as no datasets were generated or analyzed during the current study.

Declarations

Conflict of interest The authors declare that they have no conflict of interest.

References

- Amiraliyev GM, Durmaz ME, Kudu M (2018) Uniform convergence results for singularly perturbed Fredholm integro-differential equation. *J Math Anal* 9(6):55–64
- Amiraliyev GM, Durmaz ME, Kudu M (2020) Fitted second order numerical method for a singularly perturbed Fredholm integro-differential equation. *Bull Belg Math Soc Simon Stevin* 27:71–78
- Asgari Z, Toutounian F, Babolian E, Tohidi E (2019) LSMR iterative method for solving one-and two-dimensional linear Fredholm integral equations. *Comput Appl Math* 38:1–16
- Cakir M, Arslan D (2021) A new numerical approach for a singularly perturbed problem with two integral boundary conditions. *Comput Appl Math* 40:1–16
- Cimen E, Cakir M (2017) Numerical treatment of nonlocal boundary value problem with layer behaviour. *Bull Belg Math Soc Simon Stevin* 24:339–352
- Cimen E, Cakir M (2021) A uniform numerical method for solving singularly perturbed Fredholm integro-differential problem. *Comput Appl Math* 40:1–14
- Doolan ER, Miller JHH, Schilders WHA (1980) Uniform numerical methods for problems with initial and boundary layers. Boole Press, Dublin
- Durmaz ME, Amiraliyev GM (2021) A robust numerical method for a singularly perturbed Fredholm integro-differential equation. *Mediterr J Math* 18:1–17
- Ebrahimi N, Rashidinia J (2015) Collocation method for linear and nonlinear Fredholm and Volterra integral equations. *Appl Math Comput* 270:156–164
- Emamzadeh MJ, Kajani MT (2010) Nonlinear Fredholm integral equations of the second kind with quadrature methods. *J Math Ext* 4:51–58
- Farell PA, Hegarty AF, Miller JHH, O’Riordan E, Shishkin GI (2000) Robust computational techniques for boundary layers. Chapman Hall/CRC, New York
- Han C, Wang YL, Li ZY (2022) A high-precision numerical approach to solving space fractional gray-scott model. *Appl Math Lett* 125(107759):1–7
- Han C, Wang YL (2022) Numerical solutions of variable-coefficient fractional-in-space kdv equation with the caputo fractional derivative. *Fractal Fract* 6(4, 207):1–28
- Jerri A (1999) Introduction to integral equations with applications. Wiley, New York
- Liu F, Wang Y, Li S (2018) Barycentric interpolation collocation method for solving the coupled viscous burger’s equations. *Int J Comput Math* 95(11):2162–2173
- Maleknejad K, Attary M (2011) An efficient numerical approximation for the linear class of Fredholm integro-differential equations based on cattani’s method. *Commun Nonlinear Sci Numer Simul* 16:2672–2679
- Miller JHH, O’Riordan E, Shishkin GI (2012) Fitted numerical methods for singular perturbation problems. Rev. Edt. World Scientific, Singapore
- Najafi E (2020) Nystrom-quasilinearization method and smoothing transformation for the numerical solution of nonlinear weakly singular Fredholm integral equations. *J Comput Appl Math* 368:112–138
- Nayfeh AH (1993) Introduction to perturbation techniques. Wiley, New York
- O’Malley RE (1991) Singular perturbation methods for ordinary differential equations. Springer, New York
- O’Regan D, Meehan M (1998) Existence theory for nonlinear integral and integrodifferential equations. Springer, Dordrecht
- Roos HG, Stynes M, Tobiska L (2008) Robust numerical methods singularly perturbed differential equations. Springer, Berlin
- Wang YL, Liu Y, Li ZY, Zhang HL (2019) Numerical solution of integro-differential equations of high-order Fredholm by the simplified reproducing kernel method. *Int J Comput Math* 96:585–593

Publisher’s Note Springer Nature remains neutral with regard to jurisdictional claims in published maps and institutional affiliations.

Springer Nature or its licensor holds exclusive rights to this article under a publishing agreement with the author(s) or other rightsholder(s); author self-archiving of the accepted manuscript version of this article is solely governed by the terms of such publishing agreement and applicable law.